AN ULTRASTRUCTURAL STUDY OF SPONTANEOUS LUPUS NEPHRITIS IN THE NZB/BL-NZW MOUSE

ARNOLD A. CHANNING, M.D.*; TSUTOMU KASUGA, M.D.;
RICHARD E. HOROWITZ, M.D.; EDMUND L. DUBOIS, M.D.,
AND HARRY B. DEMOPOULOS, M.D.

From the Department of Pathology and Medicine,
University of Southern California School of Medicine,
Los Angeles, Calif.

An experimental model in the mouse for auto-immune disease was first suggested by the investigations of Helyer and Howie,[1,2] and Holmes and Burnet.[3] They observed the spontaneous development of hemolytic anemia associated with a circulating antibody in the New Zealand mice strains NZB/BL. Many of the animals showed glomerulopathy and a few exhibited occasional "L E" cells. When NZB/BL and NZY/BL mouse strains were mated, the F_1 and F_2 generations showed a lower incidence of hemolytic anemia. There was, however, a significant increase in the percentage of animals developing positive L E cell preparations and many developed a glomerular lesion that histologically resembled human lupus nephritis. Mating of the NZB/BL with a highly inbred white mouse, NZW, produced a generation of animals, most of which spontaneously developed progressive anemia, weight loss, hepatosplenomegaly, alopecia, skin lesions, positive L E cell preparations and nephritis. An auto-antibody was invariably present in the blood, both in the free state and bound to red cells. Conventional light microscopy of the kidney in these animals showed changes consistent with florid lupus glomerulopathy including fibrinoid necrosis and basement membrane thickening (wire-loop formation). The animals usually died of renal failure within 8 to 10 months.

Although the findings were quite intriguing, the problem posed was: Does the disease described truly represent a spontaneously developing murine version of human systemic lupus erythematosus (SLE)? The availability of a valid experimental model of SLE has significance as far as defining the etiology, pathogenesis and treatment of the human counterpart. In order to help answer this question a study of the ultrastructural glomerular alterations was undertaken in the proposed murine SLE model and results were compared with well documented ultrastructural changes in human lupus glomerulopathy.

Supported in part by a grant from the Southern California Chapter of the National Kidney Disease Foundation to Dr. Demopoulos.

Accepted for publication, May 24, 1965.

* Pathology Research Trainee.

Material and Methods

A nucleus of parent strains NZB/BL and NZW New Zealand mice was kindly supplied by Dr. J. B. Howie of the University of Otago Medical School, New Zealand. The F_1 generation of NZB/BL-NZW hybrids was carefully observed for the usual clinical features of systemic L E. After the age of 3 months, monthly blood and urine samples were obtained. Bleeding was done by puncture of the retro-orbital sinus. All blood samples were analyzed with respect to the hematocrit values, the white cell count, the presence of L E cells (using a microadaptation of the Zinkham-Conley method) [4] and with a preparation of polymerized calf DNA coated latex particles (Hyland Laboratories, Los Angeles, Calif.), the titer of antinuclear antibodies.[5] The animals were sacrificed periodically. Conventional sections were made for light microscopy. Acetone-fixed frozen sections of kidneys were treated with fluoresceinated rabbit anti-mouse gamma globulin in order to demonstrate and localize antibody globulin within the kidney. The method has been described previously.[6]

Three animals were selected at random for electron microscopic studies. Two of the mice were sacrificed at 10 months of age and the third at 14 months. Each had exhibited two plus albuminuria and repeatedly positive L E cell preparations for 3 to 4 months prior to sacrifice. Fresh kidney tissue was obtained in these 3 mice for electron microscopy. This was immediately minced and fixed in veronal acetate buffered 1 per cent OsO_4 (pH 7.4) for 1 hour at 4 to 5 degrees C. The tissue was dehydrated in the usual fashion through a series of graded ethanol solutions to absolute alcohol and finally propylene oxide. Specimens were embedded in Epon 812 and cut with an LKB-ultratome using glass knives. Thick sections were stained with toluidine blue and examined for the selection of glomerular areas. Pale gold ultrathin sections (500 Å) were made and mounted on Formvar coated no. 200 mesh copper grids and were stained with uranyl acetate. Grids were examined and photographs made using the RCA EMU-3F electron microscope at 100 KV.

Results

I. Clinico-Pathologic Summary. Approximately 70 per cent of the F_1 generation NZB/NZW mice (49 animals to date) spontaneously developed nephropathy. In a majority of the affected animals this was accompanied by anemia, proteinuria (with and without ascites), urinary casts, classic L E cells, hematoxylin bodies and antinuclear antibodies. Light microscopic examination of the kidney sections using conventional stains showed extensive glomerular alterations (Fig. 1). Glomeruli were generally more cellular with basement membrane thickening, occasional hematoxylin bodies and exhibited diffuse and verrucal fibrinoid degeneration. Treatment of kidney sections with fluoresceinated rabbit anti-mouse gamma globulin resulted in specific bright apple-green fluorescence localized in the thickened glomerular basement membranes (Fig. 2). Blocking with non-fluoresceinated anti-sera abolished such fluorescence.

II. Glomerular Ultrastructure. Examination of glomeruli by electron microscopy showed the capillary loops to be distorted and irregularly narrowed by a variable degree of mesangial, endothelial and epithelial cell swelling and an irregular deposit of highly electron-dense granular

material which generally had some topographic relationship to the capillary basement membrane (Figs. 3 to 6).

The dense deposit was present in all glomeruli examined; its quantity and exact location varied, however. Often it was intimately applied to the capillary basement membrane in a characteristic subendothelial position, but could also be found admixed within the basement membrane material, penetrating between the basement membrane and the epithelial foot processes and within the cytoplasmic matrix of both epithelial and endothelial cells (Figs. 3, 9, 11, 12 and 13). Frequently the deposit was discontinuous, even within the same capillary loop (Figs. 5, 7, 8, 9 and 13). A variation in the amount of electron-dense deposit was seen not only from glomerulus to glomerulus in the same animal, but also among capillary loops in the same glomerulus. Some loops showed little alteration except for a minimal but definite irregular and discontinuous deposition of dense material. Others were obliterated by large subendothelial deposits (compare Fig. 3 with Figs. 7 and 8). The basement membrane was more difficult to evaluate. Increased thickness of the capillary basement membrane was associated with deposits of electron-dense material, rather than an increase in size of the basement membrane itself. There was, however, a complicated bizarre network of increased basement membrane substance and varying dense deposits found throughout the swollen mesangial matrix (Figs. 3, 5, 6, 9, 10 and 11).

The epithelial cells showed variable swelling and proliferation. This was of such order that on occasion Bowman's space was obliterated (Figs. 11 to 13). The epithelial foot processes were greatly altered by reason of broadening, flattening and fusion (Figs. 4, 5, 11, 12 and 13); in some areas, however, the podocytes retained their normal size and contour. The epithelial cytoplasmic matrix often exhibited an increase in fibrillar and mitochondrial content (Figs. 5, 12 and 13).

Endothelial cells showed varied alterations. They were often swollen, with a large increase in small, smooth surfaced vesicles. Occasionally they contained electron-dense material similar to the deposits associated with the capillary basement membranes (Figs. 3, 4, 7 and 11).

The combination of swollen endothelial, epithelial and mesangial cells with the deposit of dense material contributed greatly to an appearance of obliterated, ischemic capillaries.

Discussion

In this study a hybrid strain of New Zealand mice spontaneously developed an SLE-like syndrome. Morphologic proof that the animals truly developed lupus glomerulopathy was strongly suggested by conventional light microscopic and immunocytofluorescent studies. The

ultrastructural glomerular changes, in particular the pattern of dense deposits, bore a close resemblance to those seen in human SLE nephritis.

Although human SLE is a syndrome with protean manifestations, the combination of nephritis, anemia and the presence of the L E cell phenomenon is generally sufficient for a clinical diagnosis. A serum titer of antinuclear antibodies in human cases lends further support to the diagnosis.[7-9] Moreover, the characteristic glomerular alterations (light microscopy) of lobular fibrinoid necrosis and basement membrane thickening (wire-loop formation), together with hematoxylin bodies, in human kidney are considered pathognomonic. Several investigators have shown anti-globulin fluorescence within the glomerular capillary membranes of confirmed human SLE cases and have indicated its specificity.[10-12] The proposed murine model compares favorably in regard to its clinical characteristics and renal alterations as observed by light microscopy. Aarons has recently confirmed the similarity of these changes in the murine glomerulus and has demonstrated the appearance of bright fluorescence in the glomerular basement membrane in affected mice using fluorescein labeled rabbit anti-mouse globulin.[13]

In human lupus glomerulitis, the ultrastructural changes we have seen in our own clinical material and those reported by others are characteristic.[14-16] The findings taken together are: endothelial and mesangial cell swelling, epithelial cell alterations with broadening, flattening and fusion of foot processes and the deposition of dense material on both sides of the true basement membrane, as well as within it. Electron-dense material in relationship to capillary basement membranes has been seen in human glomerular lesions unrelated to SLE, but its extent and distribution pattern is not at all like that seen in SLE. This dense material which has been labeled "fibrinoid" because of its tinctorial characteristics by light microscopy has an unusual and apparently specific pattern of deposition in human lupus nephritis. Whether or not fibrinoid is chemically related to fibrinogen, fibrin monomer or polymerized fibrin has not been definitely settled.[10-12,17] Its well-known Feulgen positivity, together with the presence of antinuclear antibodies,[18] suggest that a complex of DNA with antibody forms in capillaries, undergoes phagocytosis by endothelial cells[19] and is eventually deposited in relationship to the basement membrane.

The glomerular changes depicted in this study are similar to those seen in human lupus glomerulopathy. Alterations in epithelial, endothelial and intercapillary (mesangial) cells are essentially the same in both conditions. In addition, the pattern of dense (fibrinoid) deposit is identical to that seen in the human lesion for which it is unique.

It is apparent then that an experimental model of spontaneous SLE is

available for laboratory investigation. This has been shown by clinical, conventional histologic, immunofluorescent and electron microscopic studies. There are important immunologic and genetic implications in the elucidation of etiology and the successful treatment of SLE, but these await further investigation.

Summary

An experimental model for the laboratory investigation of human systemic lupus erythematosus has been suggested by the spontaneous development of an SLE-like syndrome in the NZB/BL-NZW hybrid mouse. In this study, approximately 70 per cent of the animals developed lupus nephropathy as measured by the classical clinico-pathologic criteria. Ultrastructural features of the lupus-like glomerulopathy were compared with the glomerular changes in human SLE. In addition to endothelial, epithelial and mesangial alterations there was a variable but constant deposition of dense material ("fibrinoid") within and on both sides of the true capillary basement membrane in the mouse observed. These features taken together are characteristic in human lupus glomerulopathy and indicate that this hybrid mouse provides a valid experimental model for SLE.

References

1. Helyer, B. J., and Howie, J. B. Renal disease associated with positive lupus erythematosus tests in a crossbred strain of mice. *Nature (London)*, 1963, **197**, 197.
2. Helyer, B. J., and Howie, J. B. Spontaneous auto-immune Disease in NZB/BL mice. *Brit. J. Haemat.*, 1963, **9**, 119–131.
3. Holmes, M. C., and Burnet, F. M. The natural history of autoimmune disease in NZB mice. A comparison with the pattern of human autoimmune manifestations. *Ann. Intern. Med.*, 1963, **59**, 265–276.
4. Zinkham, W. H., and Conley, C. L. Some factors influencing the formation of L.E. cells. A method for enhancing L.E. cell production. *Bull. Hopkins Hosp.*, 1956, **98**, 102–119.
5. Dubois, E. L.; Drexler, E., and Arterberry, J. D. A latex nucleo-protein test for diagnosis of systemic lupus erythematosus. A comparative evaluation. *J.A.M.A.*, 1961, **177**, 141–143.
6. Bauer, H.; Horowitz, R. E.; Levenson, S. M., and Popper, H. The response of the lymphatic tissue to the microbial flora. Studies on germfree mice. *Amer. J. Path.*, 1963, **42**, 471–484.
7. Miescher, P. A. Serologic reactions in systemic lupus erythematosus. *Arthritis Rheum.*, 1963, **6**, suppl., 524–535.
8. Casals, S. P.; Friou, G. J., and Myers, L. L. Significance of antibody to DNA in systemic lupus erythematosus. *Arthritis Rheum.*, 1964, **7**, 379–390.
9. Sturgill, B. C.; Carpenter, R. R.; Strauss, A.J.L., and Goodman, H. C. Antibodies in systemic lupus erythematosus and myasthenia gravis which react with thermally denatured DNA-coated Bentonite. *Proc. Soc., Exp. Biol.* Med., 1964, **115**, 246–251.

10. MELLORS, R. C.; ORTEGA, L. G., and HOLMAN, H. R. Role of gamma globulins in pathogenesis of renal lesions in systemic lupus erythematosus and chronic membranous glomerulonephritis, with an observation on the lupus erythematosus cell reaction. *J. Exp. Med.*, 1957, **106**, 191–202.

11. VAZQUEZ, J. J., and DIXON, F. J. Immunohistochemical study of lesions in rheumatic fever, systemic lupus erythematosus, and rheumatoid arthritis. *Lab. Invest.*, 1957, **6**, 205–217.

12. VAZQUEZ, J. J., and DIXON, F. J. Immunohistochemical analysis of lesions associated with "fibrinoid change". *Arch. Path. (Chicago)*, 1958, **66**, 504–517.

13. AARONS, I. Renal immunofluorescence in NZB/NZW mice. *Nature (London)*, 1964, **203**, 1080–1081.

14. FARQUHAR, M. G.; HOPPER, J., JR., and MOON, H. D. Diabetic glomerulosclerosis: electron and light microscopic studies. *Amer. J. Path.*, 1959, **35**, 721–754.

15. HOPPER, J., JR., FARQUHAR, M. G.; YAMAUCHI, H.; MOON, H. D., and PAGE, E. W. Renal lesions in pregnancy. Clinical observations and light and electron microscopic findings. *Obstet. Gynec.*, 1961, **17**, 271–293.

16. TRUMP, B. F., and BENDITT, E. P. Electron microscopic studies of human renal disease. *Lab. Invest.*, 1962, **11**, 753–781.

17. GITLIN, D.; CRAIG, J. M., and JANEWAY, C. A. Studies on the nature of fibrinoid in the collagen diseases. *Amer. J. Path.*, 1957, **33**, 55–78.

18. FREEDMAN, P., and MARKOWITZ, A. S. Isolation of antibody-like gammaglobulin from lupus glomeruli. *Brit. Med. J.*, 1962, **5286**, I, part 2, 1175–1178.

19. BROWNE, J. T.; HUTT, M. P.; REGER, J. D., and SMITH, S. W. Localization of "fibrinoid" deposit in lupus nephritis: an electron microscopic demonstration of glomerular endothelial cell phagocytosis. *Arthritis Rheum.*, 1963, **6**, 599–614.

LEGENDS FOR FIGURES

FIG. 1. A representative mouse glomerulus exhibits focal fibrinoid, basement membrane thickening and narrowing and obliteration of the capillary lumens. Hematoxylin and eosin stain. × 450.

FIG. 2. A representative mouse glomerulus shows bright fluorescence in a thickened basement membrane. Fluoresceinated anti-mouse gamma globulin. × 450.

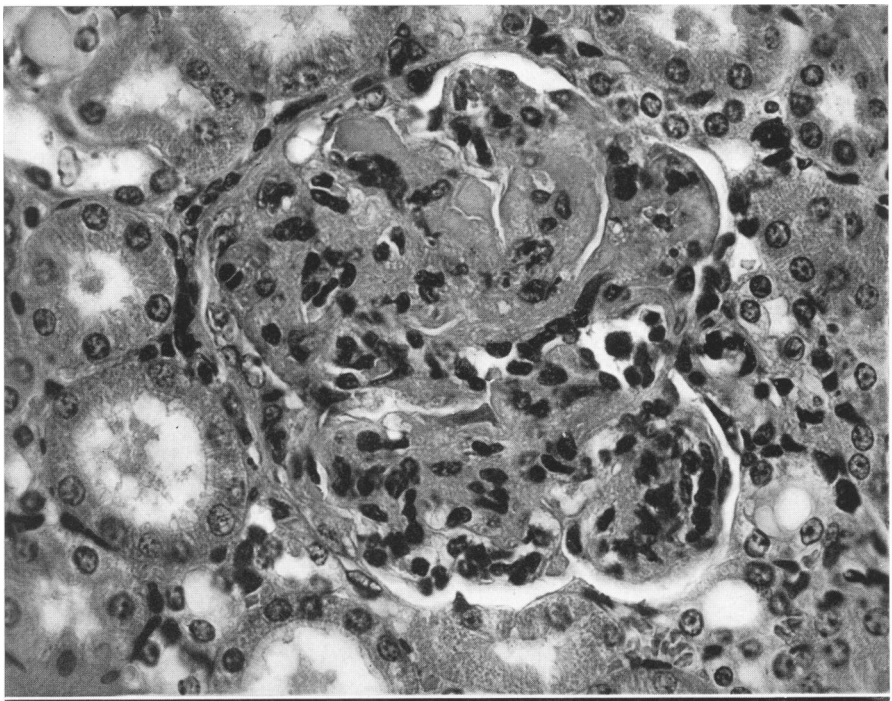

1

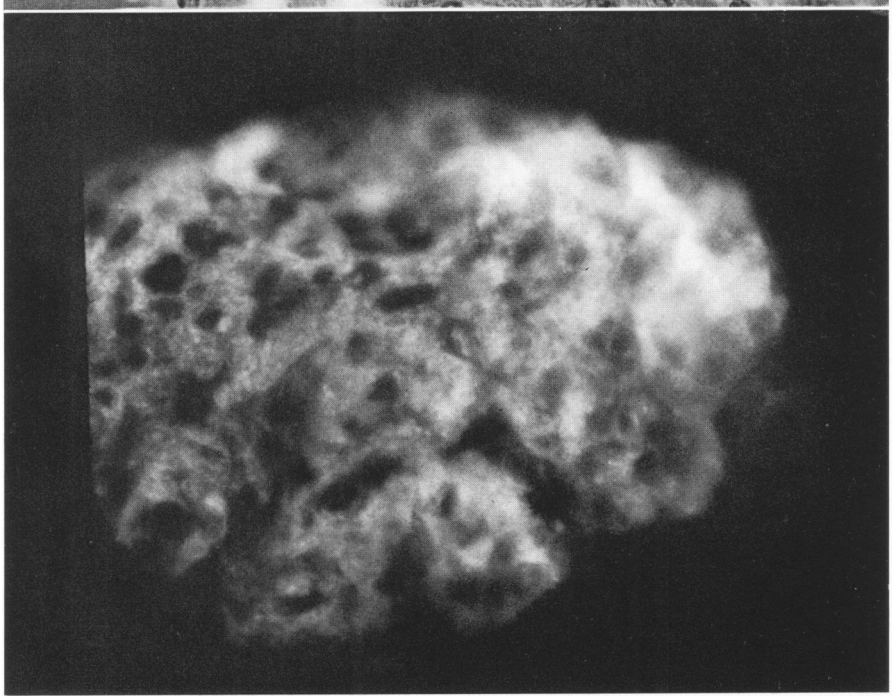

2

FIG. 3. Glomerular capillary loops exhibit a normal basement membrane (BM). The lumens are not discernible because of massive endothelial and sub-endothelial deposits of electron-dense material (DM). On the left, irregular extensions of dense material into the mesangial matrix are visible. × 6,800.

FIG. 4. Periphery of a mouse glomerulus. The capillary lumen is narrowed admitting the dimension of a single red cell (center). A swollen endothelial cell with its nucleus (N) is seen on the left. External to the capillary basement membrane (arrows) is visceral epithelium (EP) with broad flattened and fused foot processes containing electron-dense material. On the right, the visceral epithelium abuts on a basement membrane adjacent to a mesangial cell containing considerable dense deposit (DM). Bowman's space (BS); renal tubule cell (TC). × 8,000.

3

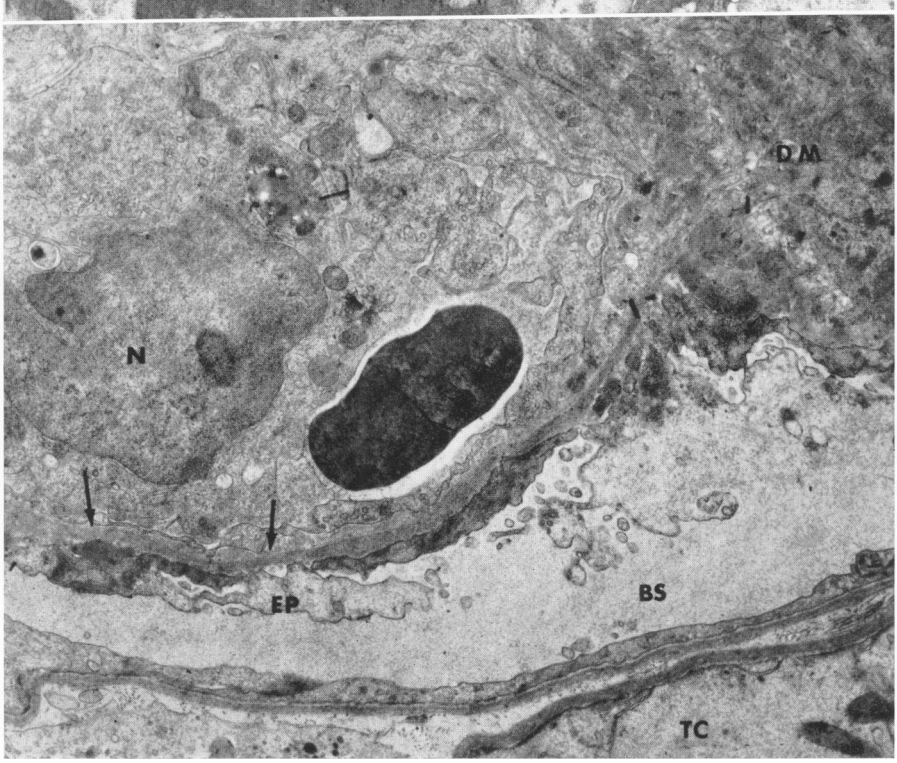

4

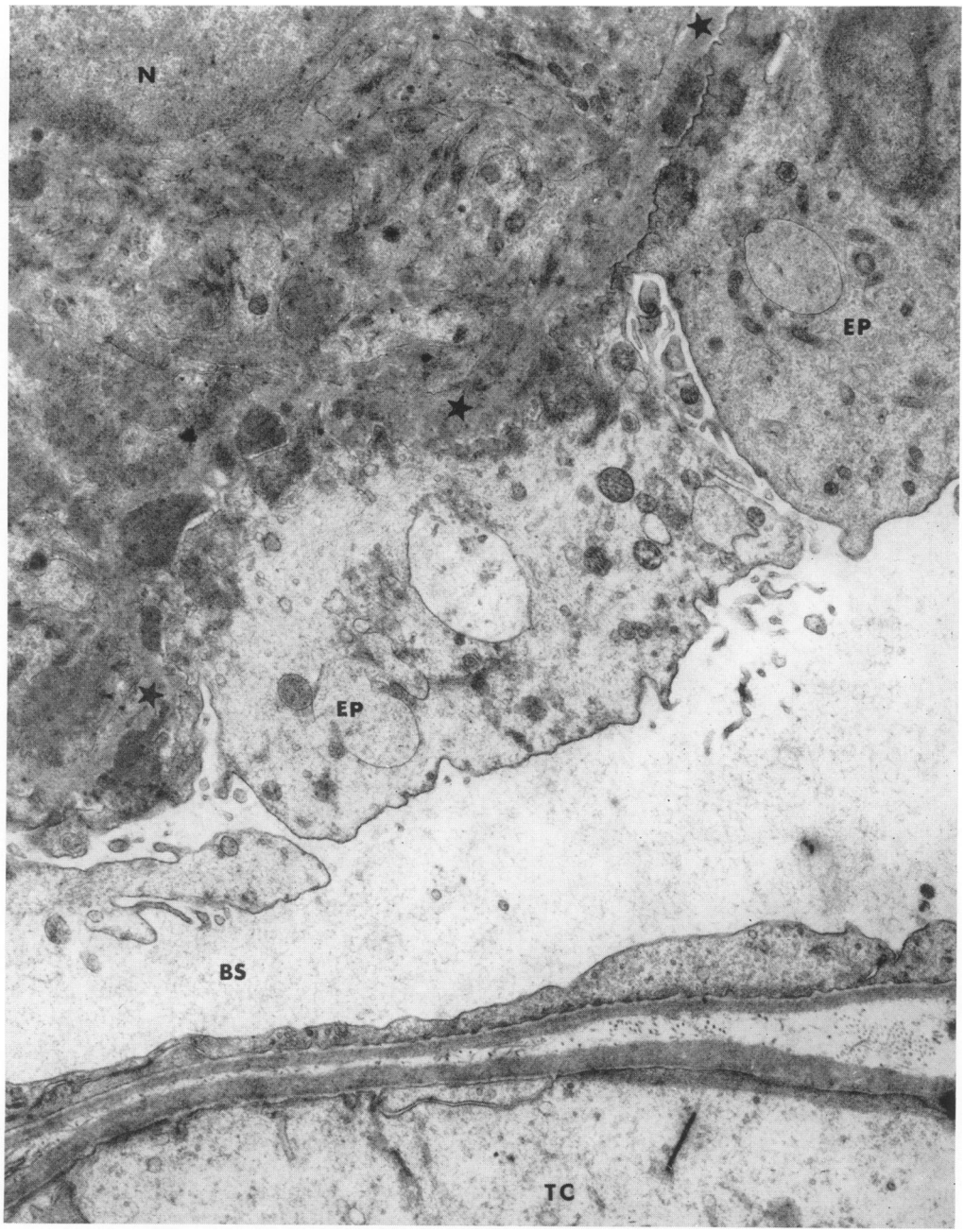

FIG. 5. An area adjacent to that shown in Figure 4. Visceral epithelium (EP) has a broad attachment to the basement membrane (stars). There is an increase in the number of fibrils within epithelial cells which also contain dense material. The latter also appears in relation to the basement membrane and is scattered throughout the mesangial matrix. Mesangial cell nucleus (N); Bowman's space (BS); renal tubule cell (TC). × 12,000.

FIG. 6. A swollen mesangial cell exhibits a complex network of basement membrane and associated dense material. On the left is a collapsed capillary. Endothelial cytoplasm (EN); mesangial cell nucleus (N). × 12,000.

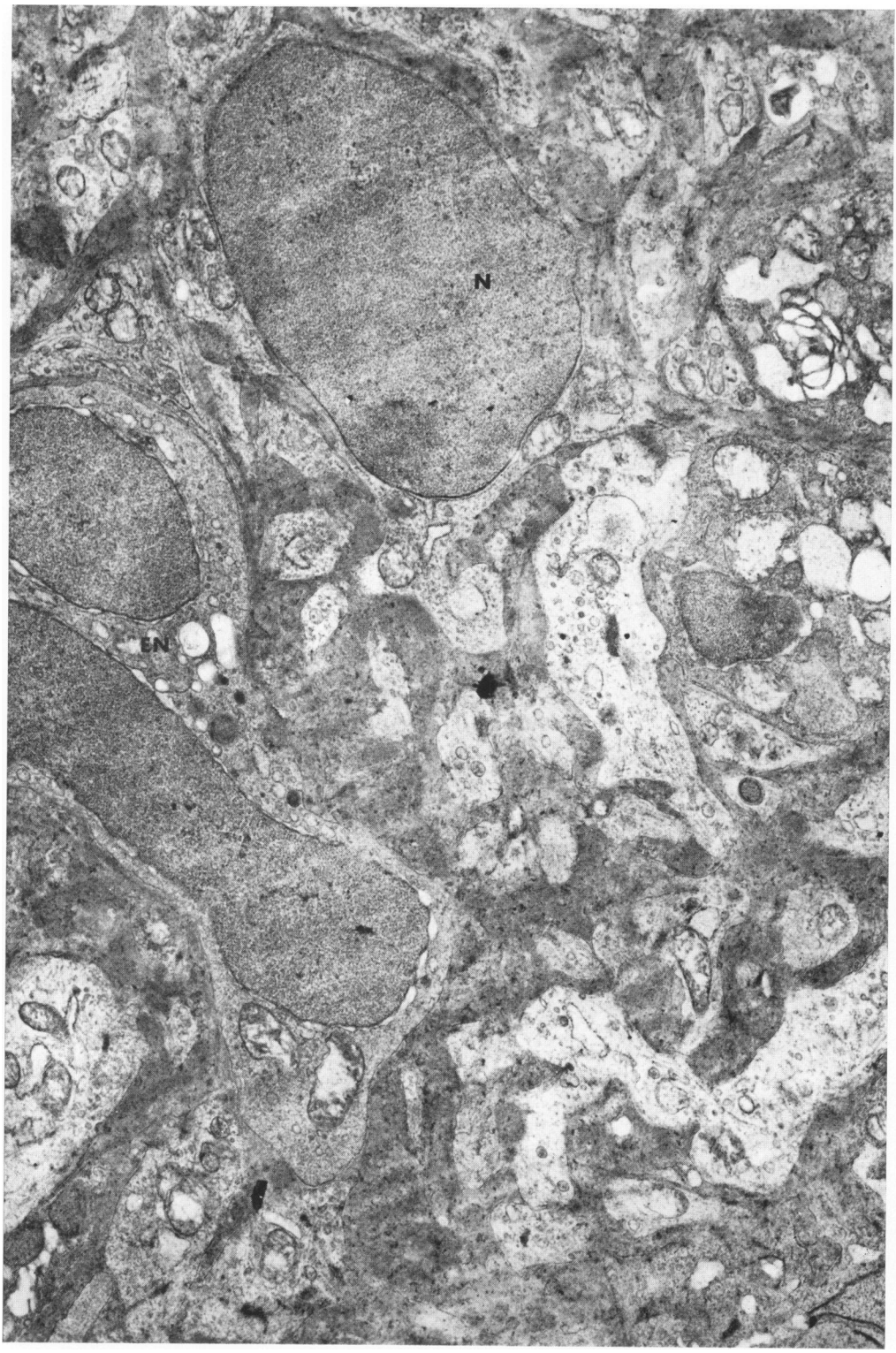

6

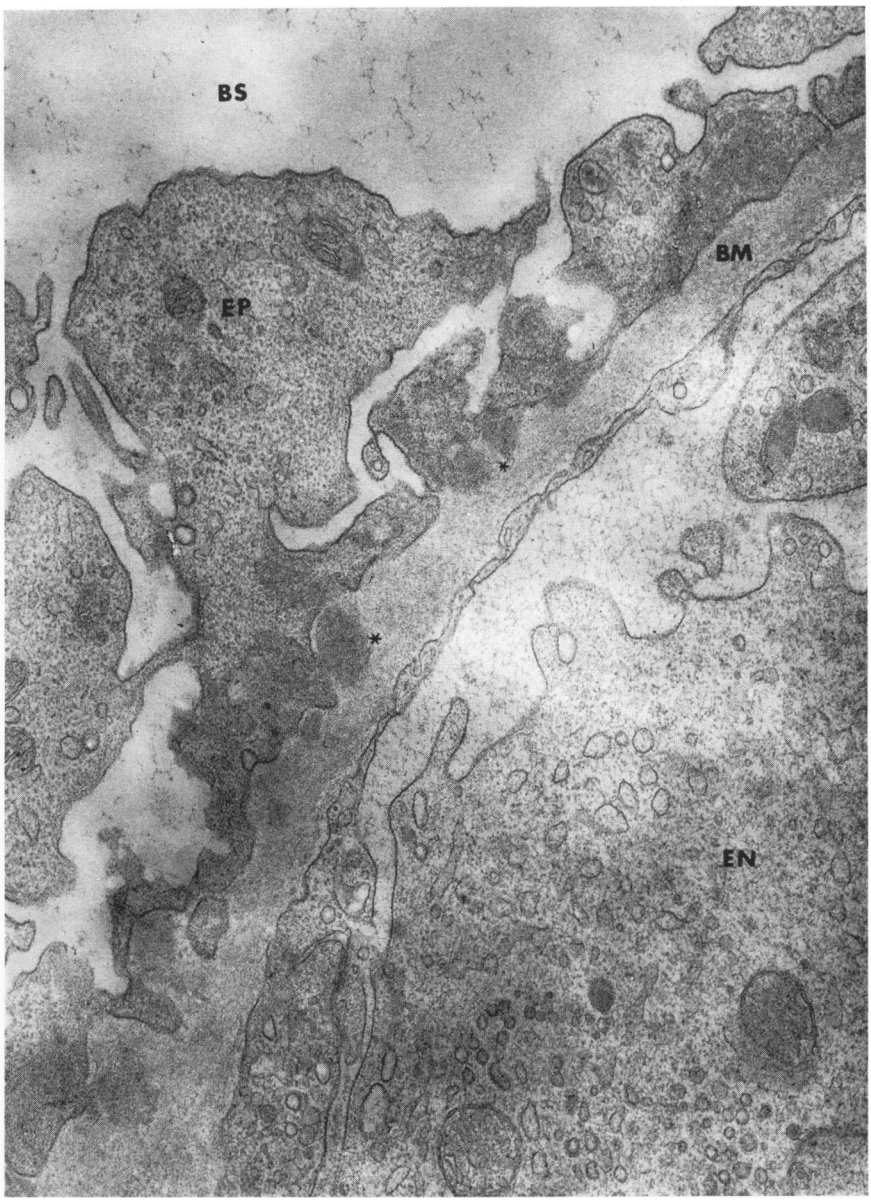

FIG. 7. A capillary loop shows a small discontinuous deposit of dense material (asterisks) within an otherwise unremarkable basement membrane (BM). The visceral epithelial (EP) foot processes are broadened and also contain deposits of dense material. Endothelial cell (EN); Bowman's space (BS). × 26,000.

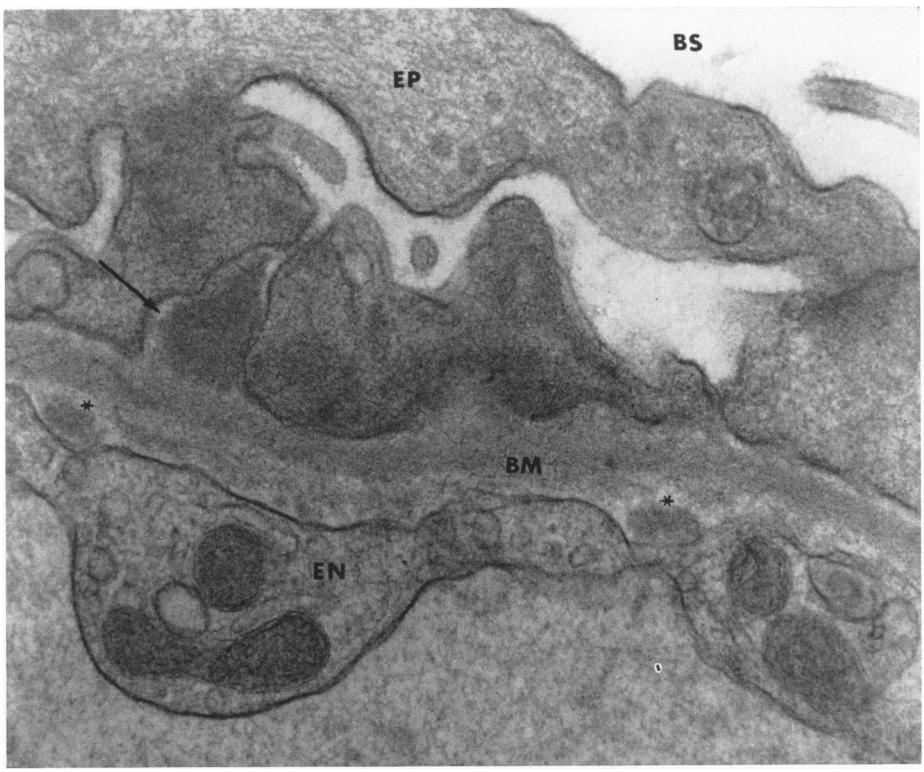

FIG. 8. A segment of capillary loop illustrates the sublety of alteration. The capillary basement membrane (BM) is not thickened. Small foci of electron-dense material (asterisks) are seen beneath the endothelium. The somewhat broadened epithelial podocytes contain some dense deposits. In one area (arrow) there is a well defined slit pore filled with dense material. Bowman's space (BS); visceral epithelium (EP); endothelium (EN). × 44,000.

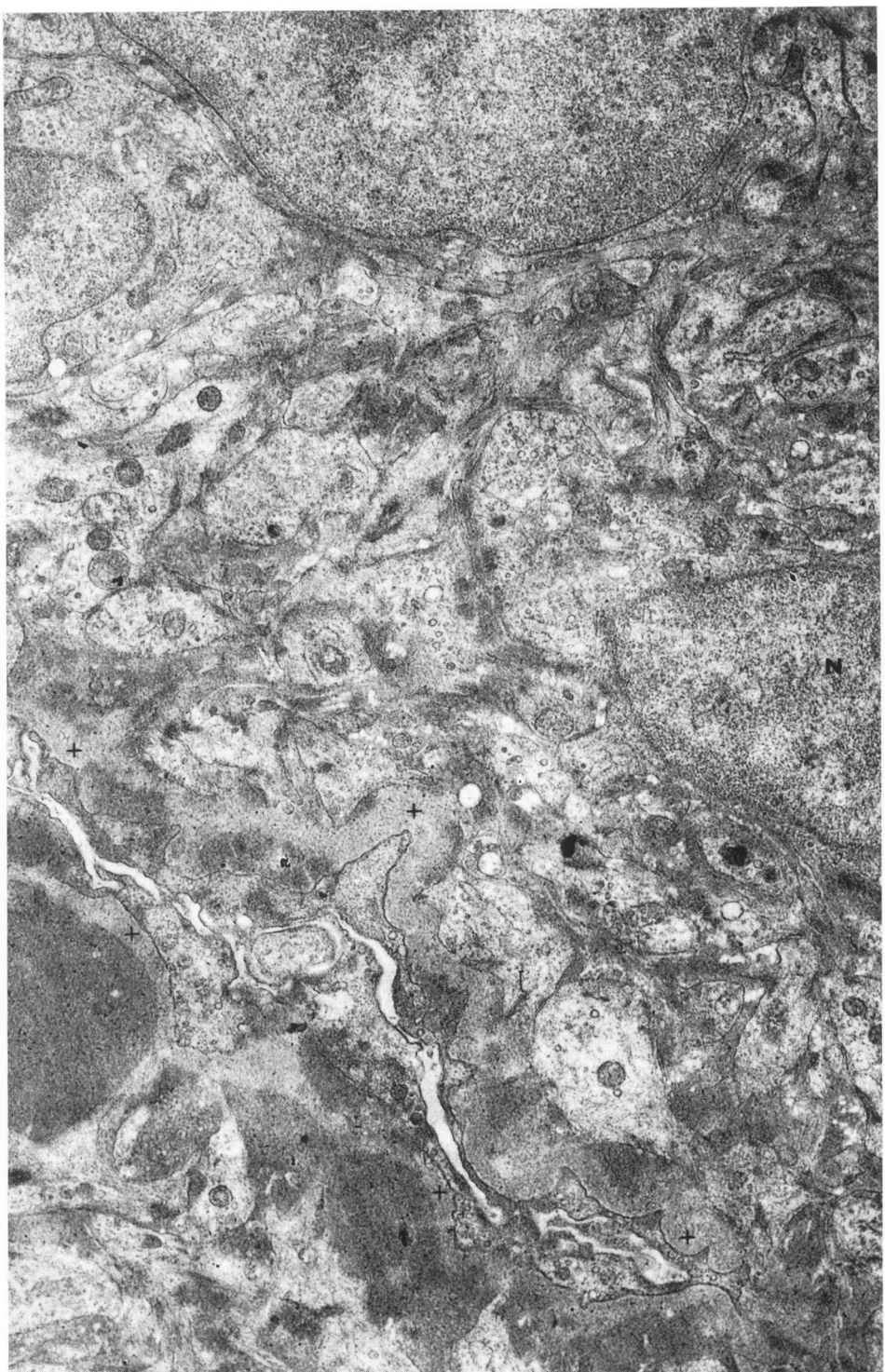

9

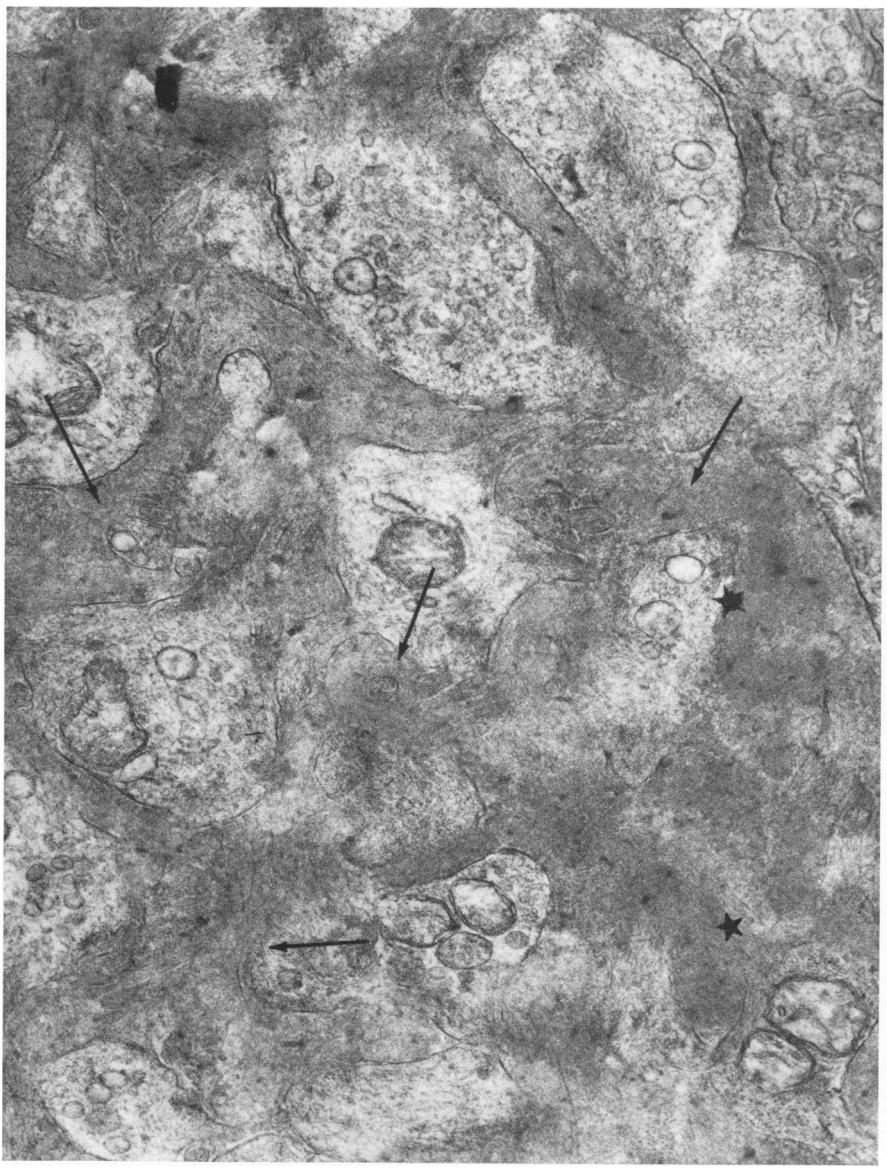

10

FIG. 9. An irregular incisura-like narrowing of Bowman's space (clear area) appears between 2 capillary loops. This results from the marked endothelial and mesangial cell swelling together with discontinuous deposits within and on both sides of basement membrane (plus sign). × 12,000.

FIG. 10. A higher power view of mesangial matrix shows a complex network of broad trabeculae (arrows) containing basement membrane and fibrillar material. Subtle electron-dense deposits are scattered throughout but are more easily seen on the right (stars). × 26,000.

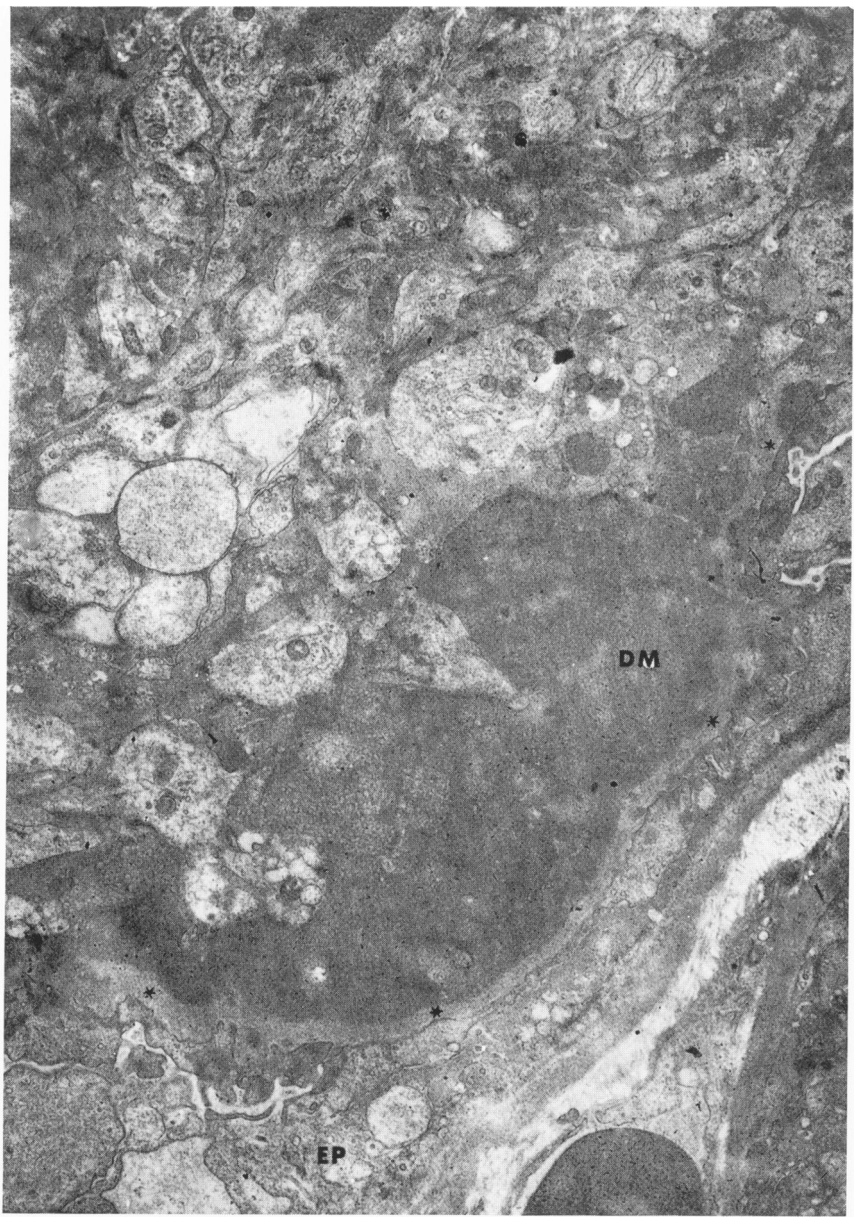

FIG. 11. Mouse glomerulus. The view shows all pathologic alterations which result in a poorly discernible Bowman's space. The capillary basement membrane (asterisks) can be traced around an essentially obliterated capillary loop. Massive deposits of dense material (DM) are found both within and beneath an endothelial cell. Additional smaller dense deposits are seen within the basement membrane and distorted epithelial cell (EP) foot processes. In the upper portion of the micrograph a trabecular network of basement membrane and dense material is seen to extend into and throughout the mesangial matrix. × 8,000.

12

FIG. 12. Marked epithelial cell (EP) alteration is associated with cytoplasmic swelling, focal deposition of dense material, fusion of foot processes and an increase in fibrils and the number of mitochondria. Membrane bound structures with multiple small vesicles are also apparent (arrows). The basement membrane (BM) can be followed around the periphery of an obliterated capillary and shows the usual varying sized deposits of dense material (DM) within it and on both sides. Endothelial nucleus (N). × 8,000.

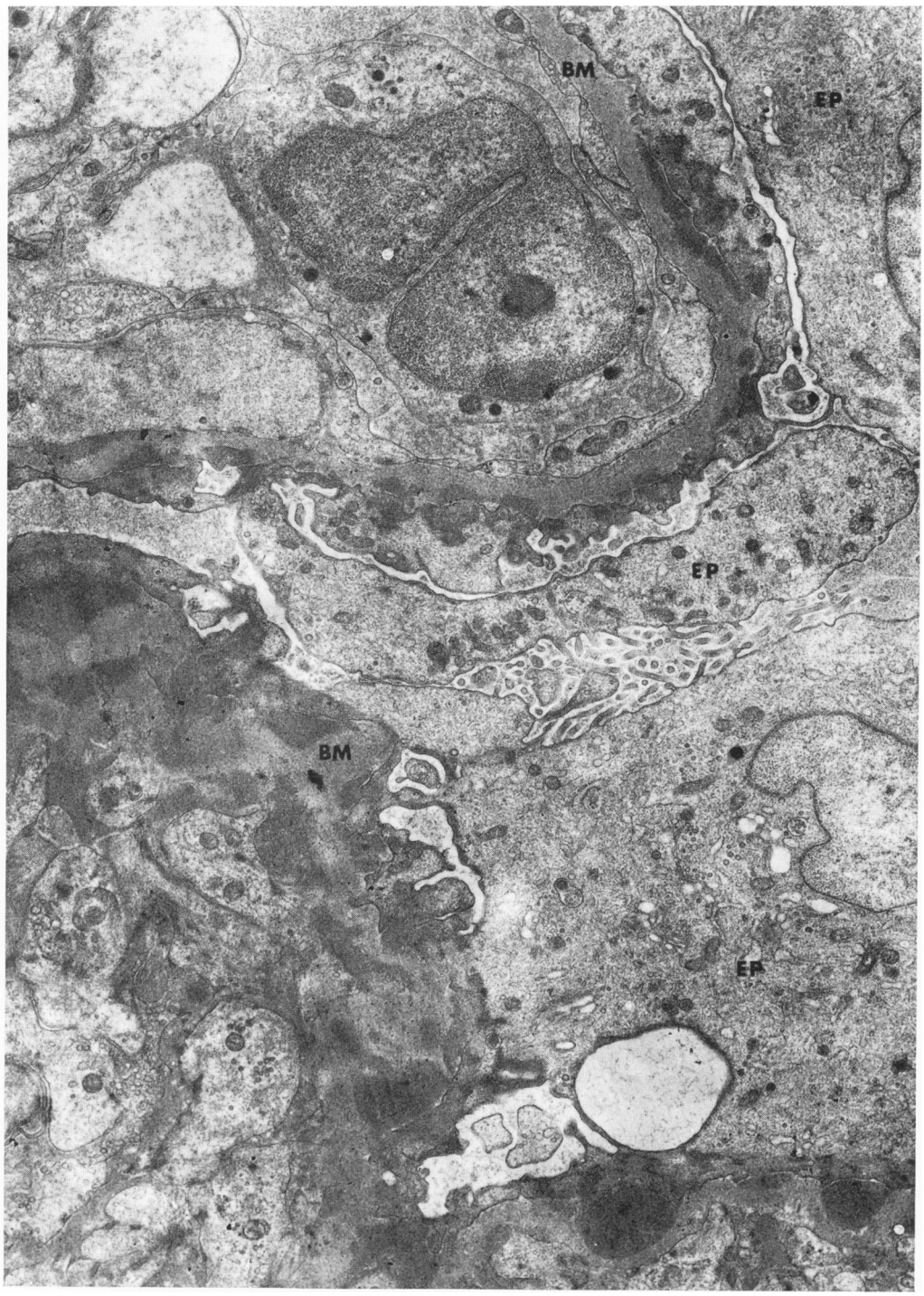

13

FIG. 13. Marked epithelial cell (EP) proliferation and swelling are evident. Membrane bound aggregates of small vesicles are scattered throughout. Portions of 2 obliterated capillaries can be delineated by following the basement membrane (BM). The same relationship of dense material to basement membrane is present as described previously. × 10,000.